

## Atmospheric corrosion of nuclear waste containers

N.P.C. Stevens, A. Cook, S.B. Lyon and J. Duff  
Materials Performance Centre, University of Manchester  
(correspondence: stuart.lyon@manchester.ac.uk)

### ABSTRACT

A combination of techniques has been used to analyse the corrosion of stainless steels under atmospheric exposure conditions. The main corrosion processes of interest are pitting and stress corrosion cracking due to the deposition of hygroscopic salts from aerosol contamination. These aerosols arise from marine spray and hence contain a mixture of sodium and magnesium chlorides. The tendency towards such localized corrosion phenomena of a metal surface contaminated by such salts depends on the degree to which the salts hydrate and form a liquid electrolyte which can support corrosion with spatially separated cathodic and anodic sites. The preparation of stressed samples for SCC tests under controlled temperatures and humidities has allowed the conditions of maximum susceptibility to be established for 304L and 316L stainless steels. The use of digital image correlation techniques allows the detection of cracking at very early stages, and allows very slow corrosion processes to be detected significantly before optical analysis by eye could detect crack growth.

### INTRODUCTION

The use of stainless steels for Intermediate Level Waste storage drums follows from the excellent compatibility between this class of materials and the cement based encapsulant materials used to provide a monolithic, high pH internal environment. With the use of passive alloys however, the risk of any local de-passivation leading to localized corrosion must be assessed. In the case of the 316L and 304L steel used for ILW drums in the UK, the most likely localized corrosion risk is that of Atmospheric Induced Stress Corrosion Cracking (AISCC) from chloride containing deposits. These can arise from marine aerosol particles of salt, which are transported very effectively in the atmosphere, and which may then deposit onto metallic surfaces and induce localized pitting, which may be followed by a transition to cracking where a requisite stress level is exceeded. These stresses may result from external loading, but more commonly arise from the forming operations to create the canisters such as cold working and welding.

As the majority of the UK nuclear plant is located near the sea, the deposition of sea salt aerosols must be considered to be likely onto any surface exposed to the atmosphere.

The use of U-Bend and 'bow-tie' samples as shown in Figures 1 and 2 has allowed the possibility of SCC at lower temperatures than

previously expected to be demonstrated for waste drum materials, as discussed at the DIAMOND 09 meeting.



**Figure 1** U-Bend samples made from sectioned 316L waste drum material exposed in a humidity cabinet. The outer top surface is stressed to the yield point, and is loaded with salt at different deposition densities by droplet deposition.

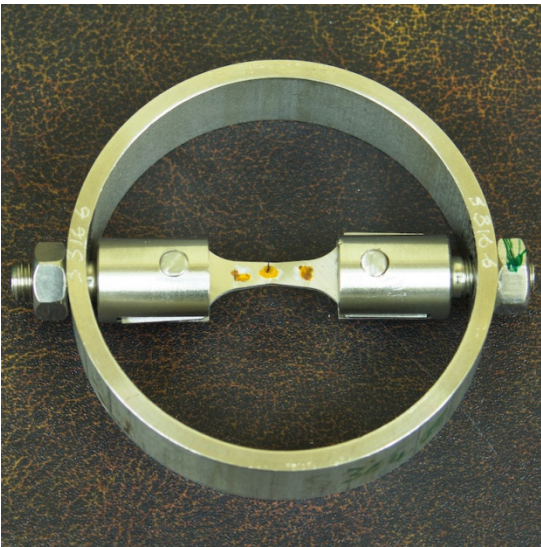
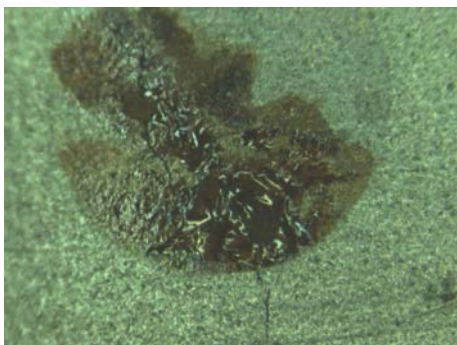


**Figure 2** 'Bow Tie' sample stressed by a proving ring, showing corrosion and cracking induced by contamination by salt droplets

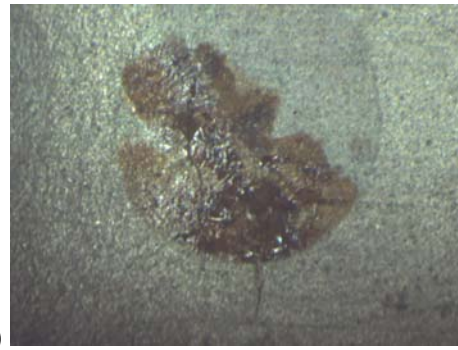
In the last year, work to look in more details at the cracking of 316L steel has continued, along with the continued development of the Digital Image Correlation technique for crack monitoring. This technique relies on the use of numerical analysis to detect the correlated movement of small features in images. By detecting difference in the magnitude of displacements across a sample surface, regions exhibiting strain and crack formation may be identified.

**CRACKING OF 316L SAMPLES**

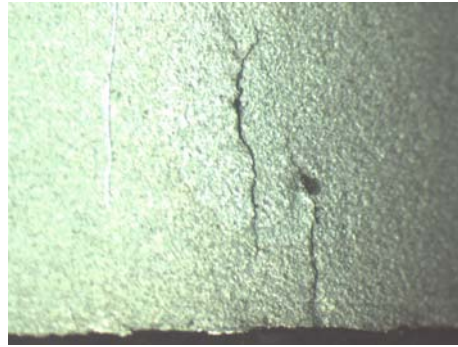
A set of 316L U-Bend samples were contaminated with  $450 \mu\text{g}/\text{cm}^2$  deposit densities of salt from a  $5 \mu\text{l}$  droplet of  $\text{MgCl}_2$ . These were then exposed in a humidity cabinet at  $40^\circ\text{C}$ , and Relative Humidity 30%, with images taken at 5 and 12 months, when the corrosion product layer was cleaned off before final imaging. This final cleaning was carried out as on some of the samples, the corrosion products formed had obscured the cracks. Figure 3 shows a sample where the transition from corrosion to cracking was relatively easy to detect, and Figure 4 shows an example where the cracks were largely obscured by the surface salt and corrosion product loading.



a)



b)



c)

**Figure 3** Top surface of 316L U-Bend sample exposed at  $40^\circ\text{C}$ , RH: 30%,  $450 \mu\text{g}/\text{cm}^2$  deposited from a  $5 \mu\text{l}$  droplet of  $\text{MgCl}_2$ , Exposure time: a) 5 months and b), c) 12 months. Stress in vicinity of crack (apex of U – bend):  $\sim 600 \text{MPa}$ . c) shows sample after oxide removal.



a)



b)

**Figure 4** Top surface of 316L U-Bend sample exposed at  $40^\circ\text{C}$ , RH: 30%,  $450 \mu\text{g}/\text{cm}^2$  deposited from a  $5 \mu\text{l}$  droplet of  $\text{MgCl}_2$ , exposed for 12 months a) before and b) after cleaning.

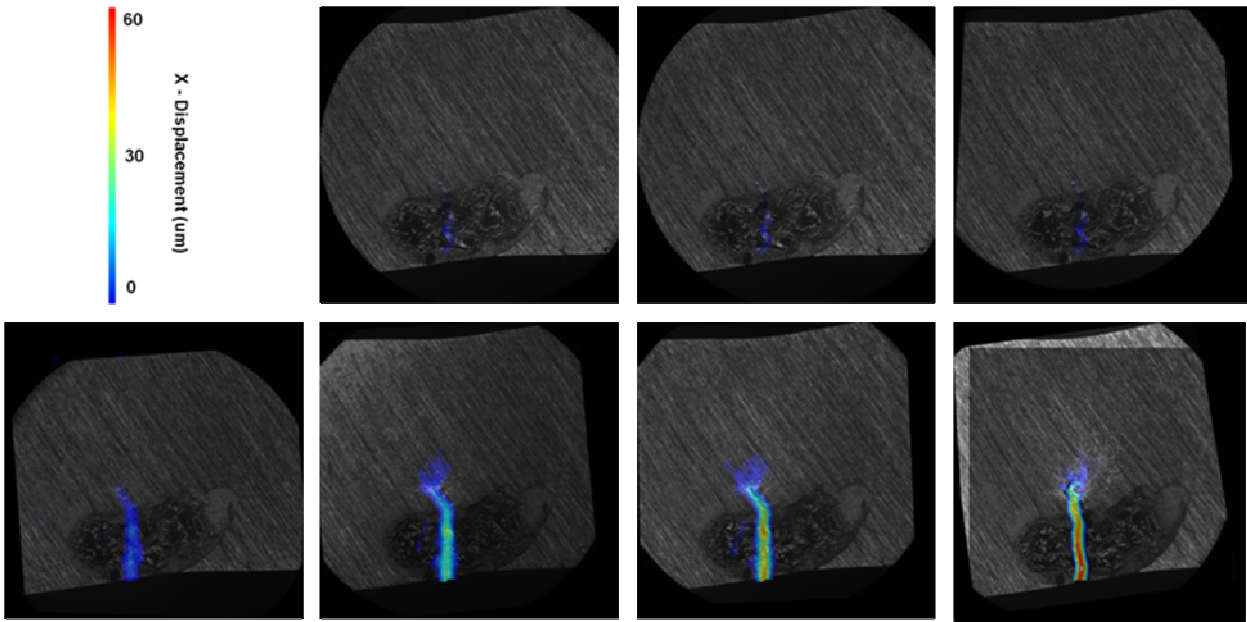


**Figure 5** Image series showing crack growth detected by DIC for SCC on a 304L tensile specimen recorded during exposure at 40°C and 30% RH at 1500 hours, 1668 hours, 1836 hours, 2004 hours, 2388 hours, 2676 hours, 3036 hours and 3232 hours (top left to lower right).

**ADVANCED DIGITAL IMAGE CORRELATION**

The use of DIC to monitor cracking processes in a qualitative way was discussed at DIAMOND 09. The facility of monitor the crack growth by measuring the crack opening allows the local behavior of cracks to be monitored, as shown in Figure 5. Using DIC to analyse the movement of regions remote from the crack itself also allows the overall relaxation of the sample to be detected. With the use of the proving ring to stress the sample, this leads to a reduction in the applied stress, The crack growth rates measured can therefore be correctly interpreted in light of the true stress and strain on the sample, as shown in Figure 6.

by modelling corresponding crack geometries to those experimentally observed.

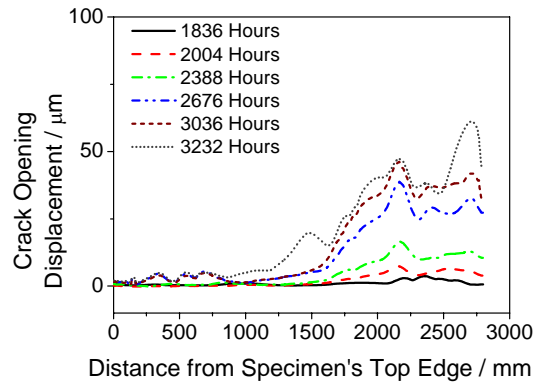


**Figure 7** Crack opening measured from sample top edge for sample shown in Figure 5

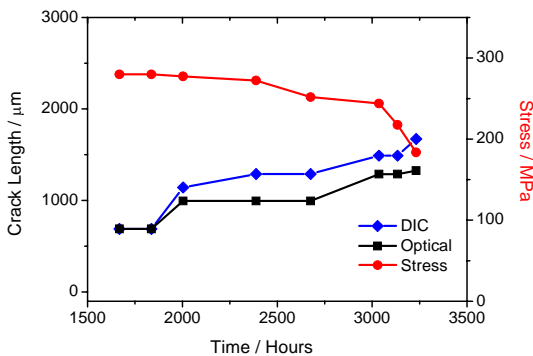


**Figure 6** Crack Length and Stress variation with time for samples shown in Figure 5

The crack opening displacements may also be extracted from the DIC analysis, and plotted as a cross section of the sample, as shown in Figure 7. This analysis offers the prospect of allowing the relationship between the mechanical force driving cracking, the stress intensity at the crack tip and the resulting crack growth rates to be investigated

**ACKNOWLEDGEMENTS**

Thanks are due to the EPSRC KNOO project and subsequently the DIAMOND consortium for funding for Tony Cook, and the Materials Performance Centre at the University of Manchester for other investigators.